

# TauSpinner: a tool for simulating CP effects in $H \rightarrow \tau\tau$ decays at LHC

T. Przedziński<sup>1</sup>, E. Richter-Wąs<sup>2</sup>, Zbigniew Wąs<sup>3,a</sup>

<sup>1</sup> The Faculty of Physics, Astronomy and Applied Computer Science, Jagiellonian University, Łojasiewicza 11, 30-348 Kraków, Poland

<sup>2</sup> Institute of Physics, Jagiellonian University, Łojasiewicza 11, 30-348 Kraków, Poland

<sup>3</sup> Institute of Nuclear Physics, PAN, Kraków, ul. Radzikowskiego 152, Kraków, Poland

Received: 19 October 2014 / Accepted: 7 November 2014 / Published online: 28 November 2014  
© The Author(s) 2014. This article is published with open access at Springerlink.com

**Abstract** In this paper, we discuss application of the TauSpinner package as a simulation tool for measuring the CP state of the newly discovered Higgs boson using the transverse spin correlations in the  $H \rightarrow \tau\tau$  decay channel. We discuss application for its main background  $Z/\gamma^* \rightarrow \tau\tau$  as well. The TauSpinner package allows to add, with the help of weights, transverse spin correlations corresponding to any mixture of scalar/pseudoscalar state, on already existing events using information from the kinematics of outgoing  $\tau$  leptons and their decay products only. This procedure can be used when polarimetric vectors of the  $\tau$ s decays and density matrix for  $\tau$ -pair production are not stored with the event sample. We concentrate on the well-defined effects for the Higgs (or Higgs-like scalar) decays, which are physically separated from the production processes. TauSpinner also allows to reintroduce (or remove) spin correlations to events from Drell–Yan  $Z/\gamma^* \rightarrow \tau\tau$  process, the main background for the Higgs parity observables, again with the help of weights only. From the literature, we recall well-established observables, developed for measuring the CP of the Higgs, and use them as benchmarks for illustrating applications of the TauSpinner package. We also include a description of the code and prepared testing examples.

## 1 Introduction

In the year 2012, ATLAS and CMS Collaborations published the discovery of a new resonance [1,2] in the search of the Standard Model Higgs boson  $H$  [3,4], with a mass of about 125 GeV. Measurement of the properties of the discovered particle [5,6] as well as tests of spin-parity quantum numbers [7,8] have confirmed hypothesis of its consistency with the Standard Model (SM) Higgs boson.

The Higgs boson decay to  $\tau$  pairs has been directly confirmed, with observed signal significance on the level of  $4.5\sigma$  (ATLAS, [9]) and  $3.2\sigma$  (CMS, [10]). The Run II of LHC, which is starting next year, will hopefully bring observation in this channel also above  $5\sigma$ .

Measurement of the Higgs CP state in the decay channel to  $\tau$ 's will be an avenue of the physics program for measuring Higgs properties in its decays to *fermions*. Tau leptons offer a unique opportunity of being excellent polarimeter probes, as the spin correlations, both longitudinal and transverse, are propagated to their measurable decay products. Availability of the multi-body decays: to single  $\pi^\pm$  or  $3\pi^\pm$ , and via resonances like  $\rho \rightarrow \pi^\pm\pi^0$ , allows to study and explore correlations between decay products.

In this paper we first recall some of the sensitive observables for the measurement of the CP Higgs boson state in the decay to  $\tau$  leptons which we will use to demonstrate functionality of the algorithm. That is why in the scope of this paper we do not review the effort for the further development of observables, such as presented in [11]. We concentrate on new developments in the TauSpinner package which can be used for studying such observables on Monte Carlo samples or data embedded events with the help of weights with easy to configure options. Both longitudinal and transverse spin correlations are now available in TauSpinner [12–14] and can be modeled with this package starting from a sample which does not include such effects. This implementation allows for simulation of transverse spin effects for the mixture of scalar/pseudoscalar Higgs boson state and also for the main background, the Drell–Yan (DY) process  $Z/\gamma^* \rightarrow \tau\tau$ . All with the help of the weights calculated after Monte Carlo samples are already generated. In particular there is no need for polarimetric vectors for  $\tau^\pm$  decays and density matrices for  $\tau$ -pair production to be stored in the event sample. For some generators such information may be made available, but not in the case of embedded  $\tau$ 's, see e.g. [9].

<sup>a</sup> e-mail: Z.Was@cern.ch

Spin correlations are introduced by spin weights  $wt$ , the kinematical configuration of each event remains intact. That is why the difference for the two cases is due to the integral of weight  $wt$ , more precisely  $(wt - 1)$ , over the whole sample. This substantially reduces statistical error. Use of weighted samples allows to study different theory models without the need of time-consuming simulation of the detector responses for arbitrary choice of Higgs parity state assumed for its decay and/or for its production matrix element. In the present paper we concentrate on Higgs decay. For scalars, decays are fully independent from the production process, which can be treated separately.

As we will show, effects from the transverse spin correlations in decays are rather small. Let us note however that the data analysis techniques which have been developed during Run I of LHC have reached unprecedented level of sophistication, both on the statistical treatment and events classification techniques. As a result, it is almost impossible to judge the feasibility to measure the Higgs boson CP with the  $\tau\tau$  decay channel. We do not address this question in our paper. But having a program available to properly model such effects will certainly be a key to the success of such difficult measurement.

Our paper is organized as follows; in the following Sect. 2, we briefly recall the definition of the longitudinal and transverse spin correlations. In Sect. 3, we recall definition of the spin-sensitive observables in the  $H \rightarrow \tau\tau$  decay. In Sect. 4, we present new development of TauSpinner package. The next Sects. 5.1 and 5.2, for signal and background respectively, collect some benchmark numerical results obtained with TauSpinner package and discuss possible improvements in the definition of those observables. Appendix A gives more technical details concerning the usage of TauSpinner. Several tests are also included to facilitate usage of the package and checks on its installation. Summary, Sect. 6, closes the paper.

## 2 Transverse spin correlations

Spin correlations of  $\tau\tau$  pairs from Higgs boson decays are sensitive to its parity [15]. This sensitivity is reflected in angular correlations of secondary decay products, in particular in the acollinearity distributions of the  $\pi^+\pi^-$  from  $\tau^+\tau^-$  decays. The spin density matrix for the two  $\tau$ s resulting from the decay of the state which is a mixture of scalar/pseudoscalar is given, using convention of [16], by the formula below

$$\Gamma(H_{mix} \rightarrow \tau^+\tau^-) \sim 1 - s_{\parallel}^{\tau^+} s_{\parallel}^{\tau^-} + s_{\perp}^{\tau^+} R(2\theta) s_{\perp}^{\tau^-}, \quad (1)$$

where  $R(2\theta)$  can be understood as an operator for the rotation by an angle  $2\theta$  (double the mixing scalar-pseudoscalar

angle  $\theta$ ) around the  $\parallel$  direction, i.e. of  $\tau^+\tau^-$  momenta in H rest-frame. The  $s_{\parallel}^{\tau^+}$  and  $s_{\parallel}^{\tau^-}$  are the  $\tau^{\pm}$  polarization vectors, which are defined in their respective rest frames<sup>1</sup> and  $s_{\parallel}$ ,  $s_{\perp}$  denotes respectively parallel and perpendicular component with respect to the  $\tau$  momenta in the H rest-frame.

The  $R(2\theta)$  spin density matrix, effectively a rotation matrix, reduces to just a diagonal one for the pure parity state:  $R_{xx} = R_{yy} = 1$  for scalar and  $R_{xx} = R_{yy} = -1$  for pseudoscalar.

## 3 CP sensitive observables

To measure effects due to Higgs parity, it is necessary to understand how effects due to the  $s_{\perp}^{\tau^{\pm}}$  component of the polarization translate to *measurable* quantities.

The  $\tau$  lepton is an unstable fermion often decaying hadronically. Such process was described for the first time in [18], its differential decay width is given by the formula

$$\frac{d\sigma}{d\Omega_{decay}} = \frac{d\sigma^{non\ polarized}}{d\Omega_{decay}} (1 + s \cdot h) \quad (2)$$

where vector  $h$  depends on the actual decay mode and its kinematical configuration, a vector  $s$  (conveniently defined in its rest-frame), parametrizes its spin density matrix, and the  $\frac{d\sigma^{non\ polarized}}{d\Omega_{decay}}$  denotes differential decay width in case when polarization is absent. In case of  $\tau^{\pm} \rightarrow \pi^{\pm}\nu_{\tau}$  the  $h$  is defined by the direction of  $\nu_{\tau}$  momentum (in  $\tau$  rest-frame). Also for other  $\tau$  decay modes  $h$  is correlated with the  $\nu_{\tau}$  momentum. The key to the measurement, used in all approaches, in particular in [16, 17, 19–22], is to have at least partial control over the relative orientation of the planes spanned by the momenta of  $\tau^{\pm}$  and its decay product  $\nu_{\tau}$  (in the Higgs boson rest-frame). Unfortunately, all these quantities are at best difficult to measure and depending on the detector conditions one of the choices may be better than other ones. The actual choice of the observable among those proposed in these references will of course depend on details of the detector and background understanding. Further improvements with respect to these references can be expected, similarly as it was the case at a time of LEP measurements, see e.g. [23] for the concept of optimal observables.

Thanks to the prolonged effort, especially in the context of preparing physics program of the future linear collider, observables sensitive to the CP spin effects were studied for final states involving  $\tau$  leptons. We would like to recall here two such observables, proposed in the literature long time ago, which are easy to interpret, but not necessarily optimized for LHC applications.

<sup>1</sup> Note the distinct frame conventions used in TauSpinner with respect to other works, e.g. Ref. [17].

In Ref. [16] it was shown that for the acollinearity angle defined in the rest frame of the Higgs boson, the shape at the end-point of the acollinearity distributions for the two pions resulting from Higgs decay can be easily interpreted as a consequence of spin parity. Reconstruction of the  $\tau$  4-momentum could be avoided, but precise control of the Higgs rest-frame was necessary. It is rather easy to understand that indeed the transverse spin correlations, carrying information on Higgs parity, can be translated into observable such as acollinearity in  $H \rightarrow \tau^+\tau^-$ ,  $\tau^\pm \rightarrow \pi^\pm\nu$  decay chain.

In Ref. [19] an alternative observable was proposed for the  $H \rightarrow \tau^+\tau^-$ ,  $\tau^\pm \rightarrow \rho^\pm\nu$ ,  $\rho^\pm \rightarrow \pi^\pm\pi^0$  decay chain. It was suggested to abandon reconstruction of the Higgs rest frame and  $\tau$  four-momenta, instead use the  $\rho^+\rho^-$  rest frame which has the advantage that it is built only from directly visible decay products of the  $\rho^+$  and  $\rho^-$ . One-dimensional angular distribution of the acoplanarity angle  $\theta_{acop}$  between  $\pi^+\pi^0$  and  $\pi^-\pi^0$  decay planes in the  $\rho^+\rho^-$  pair rest frame was proposed as CP sensitive observable. To establish this sensitivity, one has to define two categories of events depending on the sign of the energy difference between  $\pi^\pm$  and  $\pi^0$ . More specifically the energy differences are defined as follows:  $y_+$  of  $\pi^+\pi^0$  from  $\rho^+$ , and  $y_-$  of  $\pi^-\pi^0$  from  $\rho^-$  and categories depend on sign of the  $y_+ \cdot y_-$  product. Then, the distribution of the acoplanarity angle  $\theta_{acop}$  in each category separately is sensitive to the CP of the Higgs boson. Energy differences,  $y_\pm$ , as measured in the laboratory frame can be used. For better sensitivity of the observable, one can attempt to reconstruct  $y_+y_-$  in the  $\tau$ 's rest frames. The second option is however more challenging experimentally.

Also the  $\tau^\pm \rightarrow a_1^\pm\nu$  decay chain is potentially very interesting, however in this decay chain it is much more difficult to construct CP-sensitive observable that is easy to explain.

The effects of the detector resolution on the measurements of  $\pi$ 's directions and energies were already studied in [19] in context of Linear Colliders. The sensitivity to parity of the Higgs boson was preserved even if relatively large smearing was allowed, as long as the relative orientation of  $\pi^0$ 's direction with respect to  $\pi^\pm$  could be established. Precision for the measurement of energies was of no concern. Even large smearing was found not to deteriorate the CP sensitivity of the observable. It is of importance however to check, with as much experimental detail as possible, those and other observables in the LHC context (in particular observables requiring precise reconstruction of  $\tau$  decay vertex), see also [11, 22, 24].

#### 4 New development of the TauSpinner code

The TauSpinner package [12–14] represents a tool which can be used to modify  $\tau$  spin effects in samples where intermediate states decay into final states including  $\tau$  leptons.

As an input, generated samples of events featuring  $\tau$  leptons produced from intermediate state  $W$ ,  $Z$ , Higgs bosons are used. The information on the polarization and spin correlations is reconstructed from the kinematics of the  $\tau$  leptons (also  $\nu_\tau$  in case of  $W$  mediated processes) and  $\tau$  decay products alone. The hard process parton level scattering flavor/kinematical configurations, in particular  $x_1, x_2$  for PDFs, are reconstructed from the known center-of-mass energy, rapidity and virtuality of the  $\tau^+\tau^-$  pair. The convolution of the parton density functions (PDF) at given  $x_1, x_2$  and the effective Born level cross sections of the hard process can be used for calculating respective spin weights. Depending on whether longitudinal and transverse spin correlations were included in the original sample, the TauSpinner package calculates the corresponding weight, on the event-by-event basis to model the required spin effects. It allows to model spin correlations of the scalar or pseudoscalar Higgs boson or desired mixture of both states, starting from the same sample of generated events. Longitudinal spin correlations are modeled properly for the vector boson  $W$ ,  $Z$  intermediate state as well. As discussed below, the first implementation for modeling the transverse spin correlations in the  $Z$  intermediate state is also prepared in the newest version of the TauSpinner.

By calculating spin weights, attributed on the event-by-event basis, TauSpinner enables numerical evaluation of the spin effects on experimentally measured distributions and/or modification of the spin effects.

Thanks to the modularity of the design, most of the algorithms and solutions used in Tauola universal interface package [25] could have been used in TauSpinner. In Tauola universal interface longitudinal and transverse spin correlations are implemented as part of event generation since a long time. Spin effects originate directly from the properties of the matrix elements used. Because of new conditions, algorithms of Tauola universal interface<sup>2</sup> required extensions, to be useful for inserting or modifying spin effects *after-burn* on already stored events. The numerical stability of the reweighting procedure (one has to boost back  $\tau$  decay products from laboratory frame to  $\tau$  rest frames) has to be assured. In case, when information on the flavors of incoming quarks is missing in the event record,<sup>3</sup> an algorithm based on the leading-log approximation was added. This information is necessary for calculating the weights. To construct the missing information for the kinematics and/or flavor of hard process partons an additional algorithm, at present based on leading-log approximation only, had to be introduced. This is discussed in some more details in [14] and in

<sup>2</sup> In particular algorithms specific to Tauola++ universal interface [26].

<sup>3</sup> In particular for event build from embedded data.

other papers discussing TauSpinner applications [12,13]. To evaluate technical correctness of those *afterburn* algorithms it was sufficient to compare, for a given analysis selection, results from samples generated using the Tauola++ universal interface and including all effects from the beginning, with the ones where effects were obtained using the TauSpinner package. Further work, based on calculations with approximations beyond leading logarithm, will allow to improve the precision of both the TauSpinner and the Tauola++ universal interface packages. This can not be completed on the basis of programs featuring leading logarithm approximations, one may need to wait until full NLL Monte Carlo programs become available [27]. At present, comparisons with fixed order results such as [28] or with NLO simulations in particular [29,30] are planned.

#### 4.1 Transverse spin correlations in $H \rightarrow \tau\tau$ decay

The effects of transverse spin correlations resulting in sensitivity to Higgs parity in case of decays to  $\tau$  leptons was already installed in Tauola universal interface [25] some time ago.

We have discussed Higgs boson CP observability already in [19]. The method was later extended to the mixed parity case [17]. The  $\tau$  decays to two pion final states were used to present numerical results. The transverse spin correlations manifest themselves in the form of a directly observable acoplanarity<sup>4</sup> angle between (oriented)-decay planes of  $\rho^+$  and  $\rho^-$ . This observable was one of the basic benchmarks for implementing the transverse spin in Tauola++ universal interface [26], the direct continuation of ideas presented in [25].

The application of the TauSpinner package for simulating effects of the longitudinal spin correlations has been discussed in [14]. Presently, important elements of the algorithms implementing transverse spin correlations have been ported to this package. With the method of events reweighting, the algorithms are able to reintroduce correlations to the kinematics of already generated  $H \rightarrow \tau\tau$  events without those effects. This is a useful technique because it allows one to work on generated Monte Carlo events and also on the data embedded samples.

#### 4.2 Transverse spin correlations in $Z \rightarrow \tau\tau$ decay

From now on, transverse spin correlations are available with TauSpinner for the DY process,  $Z/\gamma^* \rightarrow \tau\tau$ . The spin correlation matrix  $R_{ij}$  is calculated for Tauola++ universal interface by the electroweak library [31],

including electroweak one loop corrections for the  $q\bar{q} \rightarrow Z/\gamma \rightarrow \tau\tau$  parton level production process. We have checked that, the non-diagonal part of the spin density matrix remains close to zero in high energy limit, as expected from analytic form of [32] applicable for low virtualities of  $\tau\tau$  pairs. The  $R_{xx}$  and  $R_{yy}$  components of  $\tau^+\tau^-$  pair spin density matrix (already precalculated and stored for Tauola++ universal interface in text files) are made available for the use of TauSpinner. As the actual calculation of spin weight was identical, and only parton level kinematical configuration was obtained differently, it was technically rather simple.

Let us elaborate a bit more on the actual implementations of the spin correlations.

One can represent the complete differential cross section for  $\tau$  pair production and decay as the combination of several segments. The separation into  $\tau$  decays and production components is exact, thanks to the narrow width of the  $\tau$ . Both phase space and matrix elements can be factorized into the part corresponding to production and the one corresponding to the decays. That is the property which is used in Tauola since the beginning [33]. For the cross section calculation, separation into production process and the decay is not complete, it requires introducing the spin weight  $wt$ . Only this weight depends simultaneously on kinematical variables of the production and of the  $\tau$  decays. This dependence is regular and consists of contraction of  $4 \times 4$  density matrix  $R_{ij}$  for  $\tau$  pair production and polarimetric vectors  $h_i^+$ ,  $h_j^-$  for each  $\tau^\pm$  decay. The following properties hold by construction:  $0 < wt < 4$  and  $\langle wt \rangle = 1$ . This is used in [34,35] and does not require any approximation. It is used by the Tauola universal interface and TauSpinner as well. The problem maybe be simplified however; depending on the approximations some of the components of  $R_{ij}$  may be ignored and set to zero. Also, if only collinear helicity-like degrees are taken into account, detailed definition of frames used for  $\tau$ 's quantization is not necessary.<sup>5</sup>

The  $\tau$  pair production process at LHC,  $pp \rightarrow \tau^+\tau^-X$ , can be complicated. The spectator system  $X$  can be of a very distinct type depending on the intermediate state decaying to the  $\tau\tau$  pair. For the case of Higgs production and decay, the picture simplifies since the Higgs is a narrow resonance and of a zero spin. The dominant production mode is  $gg \rightarrow H$  fusion, but independently of the production process it is enough to use Higgs decay products kinematics for calculation of the decay matrix element. For the calculation of spin weights in Tauola++ universal interface or TauSpinner, the information on four-momentum of the

<sup>4</sup> This was contrary to work [16] where difficult to measure acollinearity angle between  $\pi^+$  and  $\pi^-$  directions (in the rest-frame of Higgs) was discussed. Both  $\tau$ 's were to decay to single pion states.

<sup>5</sup> That simplifies the problem, there is no need for control on relative orientation of all quantization frames. The question of the choice of quantization frames has been discussed in detail, e.g. in Ref. [36].



Higgs, four-momenta of  $\tau$ s and their decay products are sufficient. No approximations are involved, independently of whether the transverse spin effects are taken into account or not. The production part factorizes out. Moreover the TauSpinner algorithm is designed such that modification of the production mechanism, with the help of respective weights is possible. For the case of  $2 \rightarrow 2$  processes of  $\tau$  pair production, this functionality is already available, see Ref. [13] for details.

In case of the DY process, the situation is different. Even at the lowest order information on the flavors of the incoming quarks to the hard process is needed to introduce spin correlations. This defines another segment of the calculations. In Tauola++ universal interface flavors of incoming quarks are deciphered from the history in entries of the event record. For TauSpinner, where we assume that the history in the event record is not available, four-momenta of incoming quarks are calculated from the virtuality and rapidity of the  $\tau$  pair [12]. Then, the particular quark flavor configuration is chosen randomly on the basis of PDFs (e.g. [37,38]) and quark level Born cross section. The scattering angle of the hard process is also calculated, as described in [12], following [39], and is used for calculating spin weights.

The discussion above does not exhaust all details necessary for calculation of the TauSpinner weights for spin effects discussed in this paper, but the main ingredients are explained. For more details concerning the algorithms which replace the production matrix elements with the help of weights, references [12–14] should be consulted. When adapting these algorithms for TauSpinner, we could also profit from the available corresponding segments of the Tauola++ universal interface and explore their functionalities.<sup>6</sup>

<sup>6</sup> One can use available building blocks to evaluate the properties of the background without complete simulations as well. The spin correlation matrix  $R_{ij}$  is calculated for Tauola++ universal interface by the electroweak, one loop level, segment of the code. We have started to collect the necessary preliminary results in the directory CP-tests/Z-pi. First, we have checked that, as in analytic form of [32], only diagonal parts of  $R_{ij}$  and polarization ( $R_{tz}$ ,  $R_{zt}$ ) remain non zero in the high energy limit (see the content of CP-tests/Z-pi/Rijs-INTcosthe.root file). Plots for different component of  $R_{ij}$  are given as a function of invariant mass and incoming quark flavor. The module of  $R_{ij}$  is taken and integration over the hard scattering angle is performed. Encouraged by this confirmation we have looked into the comparison of  $R_{xx}$  and  $R_{yy}$  for different values of  $s$  and incoming quark flavors but as function of the cosine of the hard scattering angle (see the content of CP-tests/Z-pi/Rijcostheta-S=2-6.root and CP-tests/Z-pi/delta12.root files). For higher values of  $s$  the  $R_{xx}$  and  $R_{yy}$  were coinciding. Thus, the resulting background will feature, see Fig. 4, transverse spin effects (necessary for CP Higgs measurement) as if the sample was not polarized, provided that the observable will symmetrize the overall orientation angle common for the two  $\tau$  decay systems, with respect to the hard scattering plane.

### 4.3 QED bremsstrahlung in decays

So far our discussion was neglecting the effects of bremsstrahlung in Higgs decay and final state radiation (FSR) in DY process. The solution to handle this effect is known and implemented in TauSpinner as discussed already in Ref. [12]. It is applicable also for observables discussed in this paper. All figures of Ref. [26] were reproduced for the samples where final state effects were included in H or  $Z/\gamma^*$  decays, no differences beyond statistical fluctuations have been observed. It is well established that bremsstrahlung effects are small and can be factorized into a separate simulation block. This required discussions of the matrix element properties and we do not plan to repeat these studies here. From the user point of view, as discussed in [12], to control the effect from final state bremsstrahlung, the intermediate state ( $H$ ,  $Z/\gamma^*$ , etc.) decay vertex has to be passed to the TauSpinner as follows. FSR photons have to be summed into the four-momentum of the intermediate state  $Z/\gamma^*$ , but not into four-momenta of  $\tau^\pm$  and their decay products. The four-momentum non-conservation of such (on-fly created) vertex will be assumed to be due to FSR photons. Detailed discussion of theoretical results behind this solution can be found in the documentation of PHOTOS [40] and references therein.

## 5 Numerical results

Below we present benchmark numerical results for the CP sensitive observables discussed above in Sect. 4. We show, that the effects of transverse spin correlations, eg. as the ones already published in [26] using Tauola++ universal interface can be reproduced using TauSpinner.

### 5.1 Case of the 125 GeV Higgs

The measurement of the acollinearity angle in the  $H \rightarrow \tau\tau$  with both  $\tau^\pm \rightarrow \pi^\pm \nu$ , which requires precise reconstruction of the Higgs rest frame, can be potentially realized in the muon collider but was considered difficult in LC or LHC experiments, due to missing neutrino momenta from  $\tau$  decays. Nonetheless, we show this observable in Fig. 1 and included it into our benchmarks discussed in Appendix A.4 because of its straightforward theoretical interpretation. Because of the simple kinematical constraints, in the rest frame of the Higgs boson,  $\tau$ 's are back-to-back and acollinearity angle, between decay products  $\pi^+\pi^-$ , essentially always is above 2.8. When zooming into this region (bottom plot of Fig. 1), a clear difference between spectra for scalar and pseudoscalar Higgs boson is observed. However,

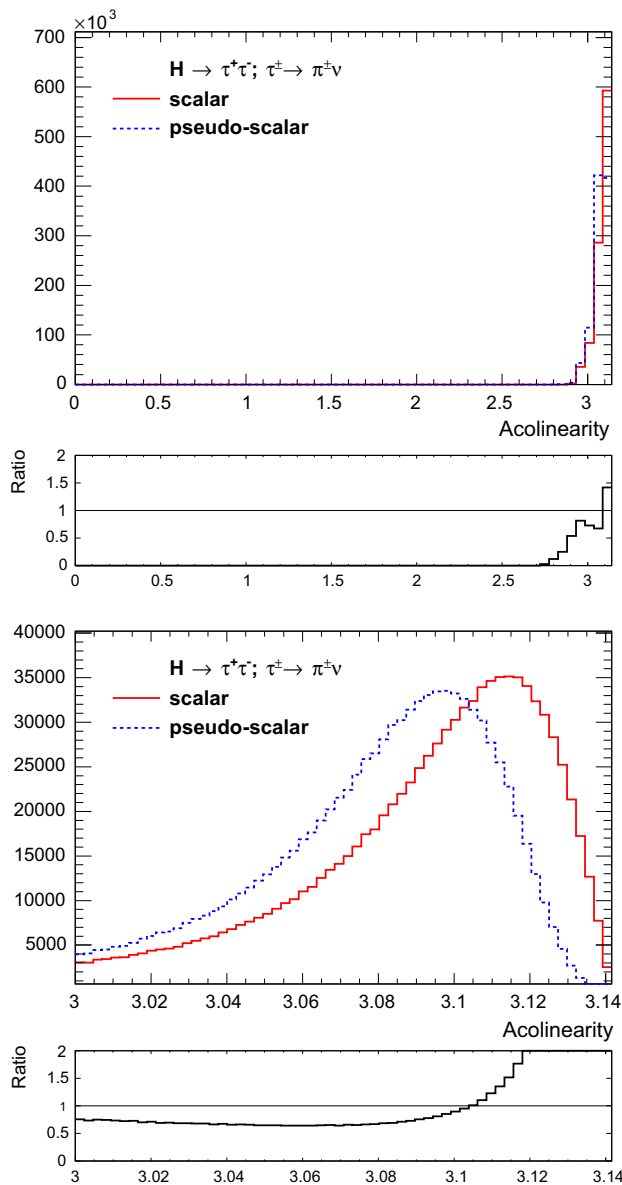


**Fig. 1** The acollinearity distributions of the  $\pi^+\pi^-$  in  $H \rightarrow \tau^+\tau^-$ ,  $\tau^\pm \rightarrow \pi^\pm \nu$  decays. Red line corresponds to the scalar and blue dashed line to the pseudoscalar case. Black line shows the ratio of the distributions. On the bottom, the acoplanarity range is zoomed to show its endpoint region. There is no difference for this distribution for 8 or 14 TeV center of mass energy pp scattering

to measure it experimentally, very precise reconstruction of the Higgs boson rest frame would be mandatory.

We consider the  $H \rightarrow \tau^+\tau^-$ ,  $\tau^\pm \rightarrow \rho^\pm \nu$ ,  $\rho^\pm \rightarrow \pi^\pm \pi^0$  decay chain and one-dimensional angular distribution of the acoplanarity angle  $\theta_{acop}$  between the  $\pi^+\pi^0$  and the  $\pi^-\pi^0$  decay planes in the  $\rho^+\rho^-$  pair rest-frame (Ref. [19]). In view of the Standard Model Higgs boson of a mass of 125 GeV, it is a good candidate for a CP sensitive observable at LHC.

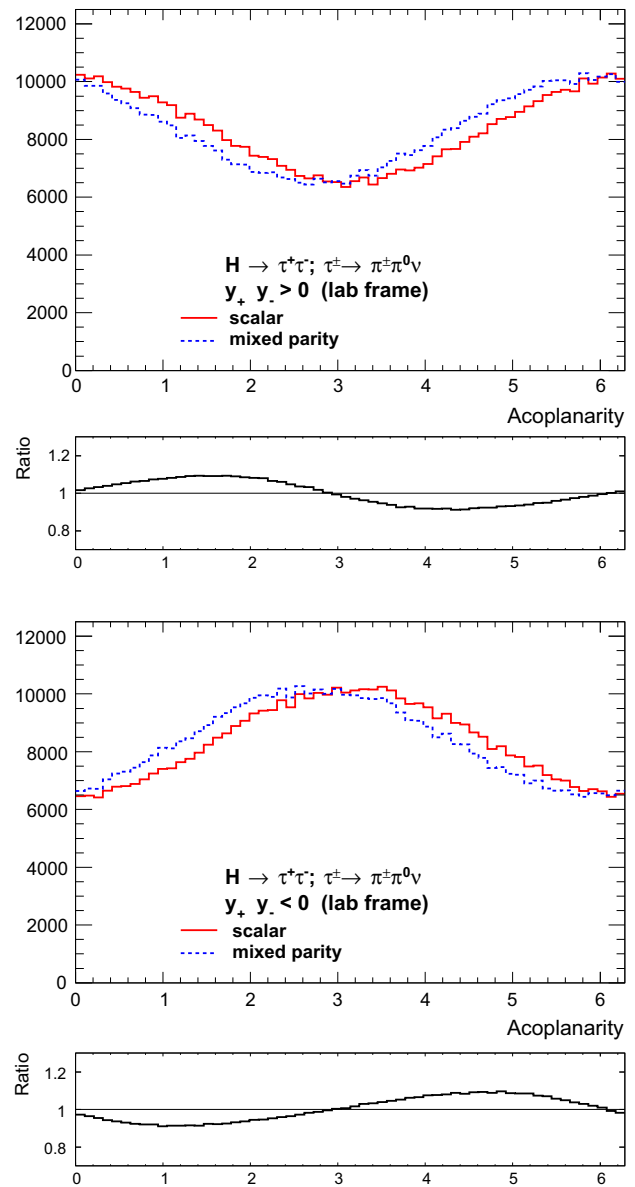


**Fig. 2** The acoplanarity distribution for the  $H \rightarrow \tau^+\tau^-$ ,  $\tau^\pm \rightarrow \pi^\pm \pi^0 \nu$  decays calculated in the  $\pi^+\pi^0\pi^-\pi^0$  rest frame (see text for more details). Top plot for events with  $y_- \cdot y_+ > 0$ , bottom plot for  $y_- \cdot y_+ < 0$ . Compared are scalar (red) and mixed scalar-pseudoscalar (blue dashed), with mixing angle  $\theta = 0.2$ , cases. The  $y_\pm$  variables are calculated in the laboratory frame. There is no noticeable difference for this distribution for 8 or 14 TeV center of mass energy of pp scattering. This is the case of all our further figures as well

This distribution is CP sensitive if events are separated<sup>7</sup> into two categories, accordingly to the sign of the product  $y_+ \cdot y_-$ .

We recall this distribution<sup>8</sup> in Fig. 2. We split events into two separate categories and compare the case of the scalar

<sup>7</sup> This separation, thanks to the properties of  $\tau$  decay matrix elements, correlates the  $\rho$  decay plane with the one spanned on  $\tau$  and  $\nu_\tau$  momenta.

<sup>8</sup> Details on the program used in preparation of this plot are given in Appendix A.4.

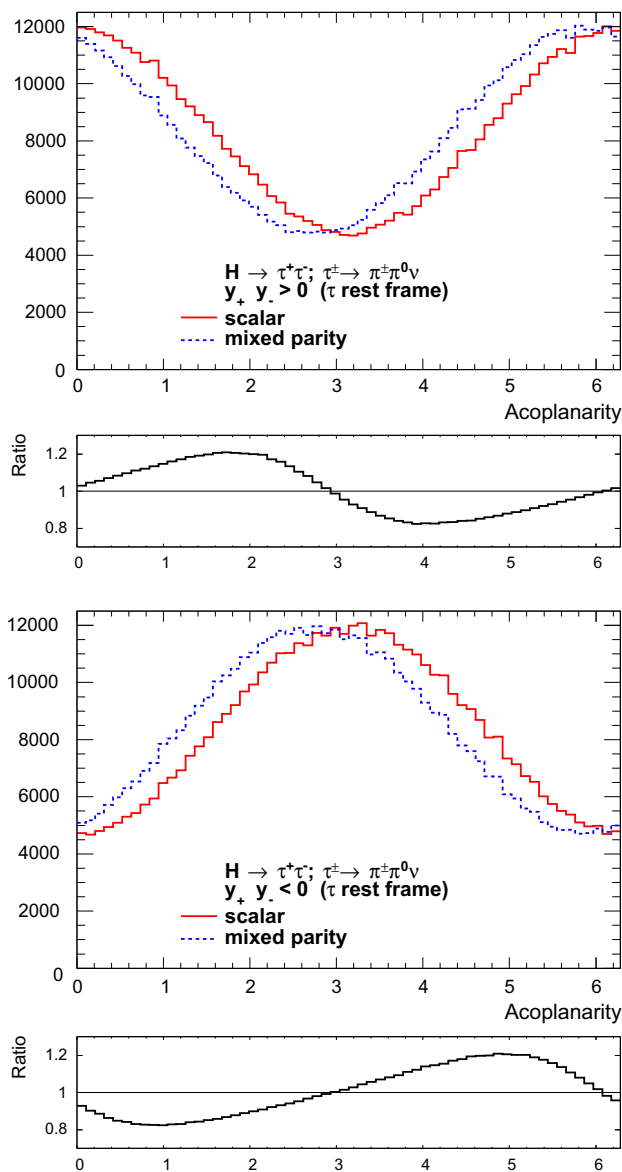


**Fig. 3** The same as Fig. 2 but with  $y_{\pm}$  variables calculated in  $\tau^{\pm}$  rest frames. The acoplanarity angle is always calculated in the  $\pi^{+}\pi^{0}\pi^{-}\pi^{0}$  rest frame

(red) and the mixed scalar-pseudoscalar state (blue dashed) with assumed mixing angle  $\theta = 0.2$ . The  $\theta_{acop}$  distribution relies on measurement of the four-momenta (in the laboratory frame) of the  $\pi^{+}\pi^{0}$  and  $\pi^{-}\pi^{0}$  only. No reconstruction of the rest frames of Higgs and/or  $\tau^{\pm}$  is required. Obviously, the nature of the observable is at least three dimensional and the multi-dimensional fit in the space  $(\theta_{acop}, y_{-}, y_{+})$  offers additional increase in sensitivity of this measurement.

Figure 3 shows the same distribution but when  $y_{\pm}$  energy differences are calculated in  $\tau^{\pm}$  rest frames instead of the laboratory frame. Reconstruction of  $\tau^{\pm}$  rest frames can be in part achieved with the help of  $\tau$  decay vertex measurement.

Comparison of Fig. 3 and Fig. 2 allows to estimate available potential improvement which may be accessible also at LHC.

This optimization can be realized in part, if the  $\tau$  decay vertex is measured to a limited precision, as used in [20]. This helps resolving twofold ambiguity in reconstructing the  $\tau$  momentum. Other examples where the reconstruction of the decay vertex is used as an essential part of the observable, are given in [21] and also<sup>9</sup> in Ref. [41]. Naturally, extension to other decay modes of  $\tau$ 's, especially to  $3\pi$  channels will be beneficial as well. These channels offer substantial increase of the sample statistics, and also, if ignored would contribute to the background. Many options, with optimal choices depending on details of detector response, the hard scattering and  $\tau$  decay distributions, can be envisaged.

## 5.2 Case of Drell–Yan background

Studies of the transverse spin effects and of CP sensitive observables can not be completed for the Higgs boson unless properties of the main background, that is DY  $Z/\gamma \rightarrow \tau^{+}\tau^{-}$ , are studied as well. At LHC, this dominant background is difficult to separate from the Higgs boson signature [9]. Both ATLAS and CMS use embedded  $\tau$  samples for the estimation of this background [9, 10]. Control of the transverse spin effects can be realized in this case with the help of weights of the new version of TauSpinner presented in this paper.

Numerical results for the DY sample with  $m_{\tau\tau} > 60$  GeV are shown in Fig. 4, for the acoplanarity of the  $\pi^{+}\pi^{-}$  directions, i.e. the same variable as in Fig. 1 for the Higgs boson. Note that because of the line-shape of the  $Z/\gamma^{*}$ , i.e. large spread of the  $\tau^{+}\tau^{-}$  virtualities, the end-point of the  $\pi^{-}\pi^{+}$  acollinearity distribution is not as sharp as for the Higgs boson. For DY events, no transverse spin effects can be seen (bottom plot). To nevertheless enhance effects from the spin correlations, an additional cut on

$$|\cos \theta_{planes}| > 0.5 \quad (3)$$

is introduced (top plot), leading to a difference of 20 % in the shape of the falling edge. The  $\theta_{planes}$  is an angle between planes defined by:  $\tau^{\pm}$  momentum – beam momentum (first plane) and  $\tau^{\pm}$  momentum and its decay product  $\pi^{\pm}$  momentum (second plane).

<sup>9</sup> Note that the angles  $0 < \phi^{*} < \pi$  and  $0 < \Psi_{CP}^{*} < \pi$  of Ref. [41] are related to our angle  $0 < \theta_{acop} < 2\pi$ . The  $\phi^{*} = \arccos(\cos(\theta_{acop}))$  and  $\Psi_{CP}^{*} = \arcsin(\sin(\theta_{acop}))$ . Different, but correlated, physics input is used for the definition of planes. In Ref. [17] planes spanned on momenta  $\pi^{\pm}$  and  $\pi^{0}$  from  $\rho^{\pm}$  decays are used. In [41] the plane spanned by  $\tau$  direction and its charged decay product is used instead; exactly as the angle  $\phi^{*}$  of Ref. [16]. The actual choice will depend on how well measured are  $\pi^{0}$  directions and precision of reconstruction of the  $\tau$  decay vertex. If all these quantities are to be shown to be measurable, one should consider simultaneous fit to multidimensional distribution over all of the variables.

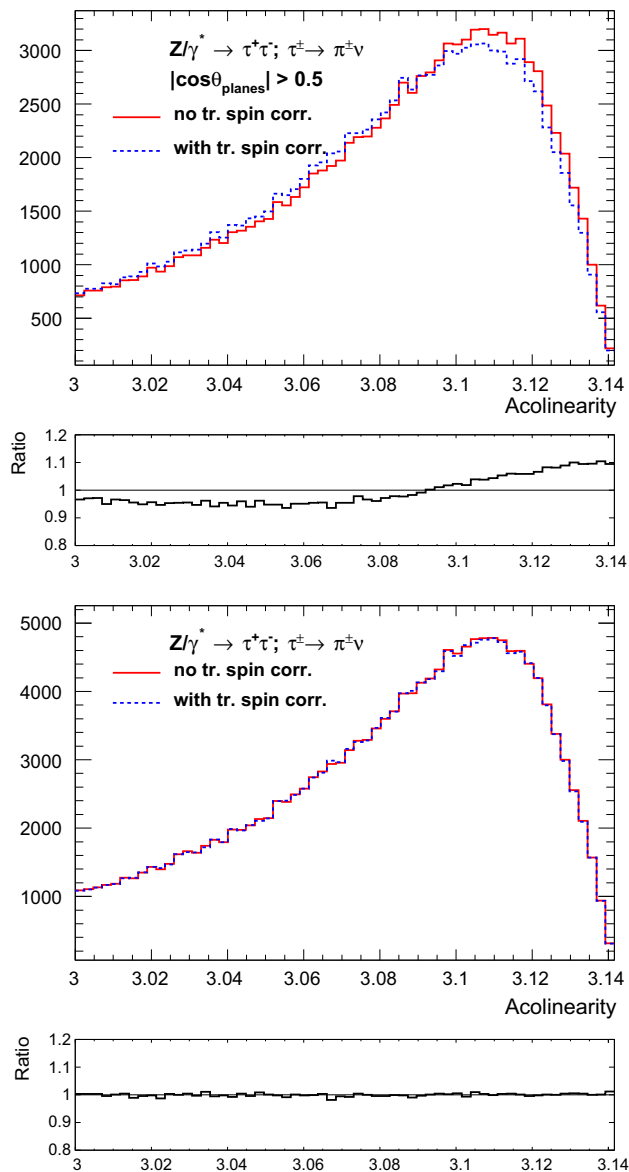


**Fig. 4** The acollinearity of  $\pi^+\pi^-$  directions in the rest frame of intermediate  $Z/\gamma^*$  state, invariant mass of the  $\tau^+\tau^-$  pair is requested to be larger than 60 GeV. An additional cut has been applied (*top plot*), as defined in the text, to enhance effect from transverse spin correlations. Without this cut (*bottom plot*) effect is substantially smaller than statistical fluctuations

The DY background is also characterized by a simply flat distribution of the acoplanarity angle, in case of  $Z \rightarrow \tau^+\tau^-$ ,  $\tau^\pm \rightarrow \rho^\pm \nu$  decay chain; where  $\theta_{acop}$  is defined between  $\pi^+\pi^0$  and  $\pi^-\pi^0$  decay planes in the  $\rho^+\rho^-$  pair rest frame. The distribution, shown in Fig. 3 for the Higgs case, becomes a sensitive observable only if dependent on the sign of  $y_- \cdot y_+$ . This is not the case of the Z boson (independent of the sign of  $y_- \cdot y_+$ ) and this feature may be used to control the background, unless (unlikely) destroyed accidentally by some selection cuts.

We have cross-checked these results with samples generated including transverse-spin correlations directly (i.e. using Tauola++ universal interface). In this case, the transverse spin effects for the DY production are activated simultaneously with the electroweak loop corrections, see [26].

## 6 Summary

In this paper, we have presented a new extension of the TauSpinner package, namely the implementation of the transverse spin correlations in the decay of scalar/pseudoscalar state into a pair of  $\tau$  leptons as well as for DY  $Z/\gamma^*$  processes. The *afterburn* modeling of the correlations is achieved by calculating weights on the event-by-event basis using only information on the kinematics of the outgoing  $\tau$  decay products. This provides a convenient tool, where multiple models can be studied on the correlated events without the need for CPU-intensive simulations. The question of weights to model/replace matrix elements used for generating scalar/pseudoscalar state production is postponed to a forthcoming paper.

The new functionality has been achieved by porting and adapting code developed for the Tauola++ universal interface package, so it can be used on already generated events where such correlations were included or not.

We have recalled two observables sensitive to the transverse spin correlations in case of  $H \rightarrow \tau\tau$  decays, which have been proposed already some time ago: acollinearity in case of  $\tau \rightarrow \pi^\pm$  decay, and acoplanarity in case of  $\tau \rightarrow \pi^\pm \pi^0 \nu$  decays. They have been used to provide numerical benchmark of this implementation, for the Higgs mass of 125 GeV, as recently discovered by the LHC experiments.

We have also discussed transverse spin correlations for the DY  $Z/\gamma^*$  background process, which can now be modeled with the TauSpinner package. We have shown that the effect for background is marginal (as expected for our distributions). Nevertheless, given the fact that experimental selection may enhance such effects it is considered as important to have it also available. See e.g. [42].

We have not addressed here the question of the feasibility to observe transverse spin correlations in the analyzes of  $H \rightarrow \tau\tau$  channel at LHC. Given nowadays very refined analysis techniques, even rather small effects can be turned into successful measurements. Our aim was to prepare, describe and validate a tool which may be useful for such a goal.

We have concentrated on the Higgs decays. One expects that for the distinct parity of the Higgs-like object, its production hard scattering matrix element should differ as well. Respective modifications to the production matrix elements of the user choice (and not only to the spin correlation weight discussed in the present paper) has been implemented for the



$2 \rightarrow 2$  hard processes since some time now [13]. Our plan now is to extend this functionality also to the vector boson fusion production processes [43], that is kinematical configurations of final states consisting of  $\tau^+\tau^-$  pair and two jets. Implementation of the transverse spin effects, for user provided non-standard physics processes, may be considered in the future as well.

**Acknowledgments** This research was supported in part by the Research Executive Agency (REA) of the European Union under the Grant Agreement PITN-GA-2012-316704 (HiggsTools) and by funds of Polish National Science Centre under decision DEC-2011/03/B/ST2/00107.

**Open Access** This article is distributed under the terms of the Creative Commons Attribution License which permits any use, distribution, and reproduction in any medium, provided the original author(s) and the source are credited.  
Funded by SCOAP<sup>3</sup> / License Version CC BY 4.0.

## Appendix A: TauSpinner technical details

This applies to Tauola tar ball starting from version 1.1.5 (TauSpinner version 1.4.0).

Further details are given in the following sections and in README files of the distribution tar-ball. All the plots of the present paper can be reproduced with the help of new demonstration programs which are included in the Tauola++ v1.1.5 (or later) distribution tar-ball. We are using the ROOT-based MC-TESTER package [44] to facilitate histogramming and plotting.

### A.1 Initialization

In case of transverse spin effects, the following changes have to be introduced for TauSpinner initialization. The rest of its execution is performed as explained in the previous publications [12, 13]. In particular, all weights will still be calculated by calling the function `calculateWeightFromParticlesH`.<sup>10</sup>

Let us give a few details concerning different options:

#### Case of Higgs bosons

- At initialization stage:  

```
setHiggsParametersTR(-1.0, 1.0, 0.0, 0.0);
```

for scalar Higgs or  

```
setHiggsParametersTR( 1.0, -1.0, 0.0, 0.0);
```

for pseudo-scalar Higgs

<sup>10</sup> For the purpose of adding new functionality, TauSpinner must access private fields and functions of `TauolaParticlePair` class from Tauola++ universal interface library. This has been resolved through a proper friend declaration in `TauolaParticlePair.h` header file. No other modifications were needed.

- For mixed parity state, use:  

```
double theta = 0.2;
setHiggsParametersTR(-cos(2*theta),
cos(2*theta), -sin(2*theta),
-sin(2*theta));
```

Note distinct sign convention, see footnote 1.

#### Case of DY process

- At initialization stage:  

```
setZgamMultiplierTR(1.0, 1.0, 1.0, 1.0);
```

the  $R_{xx}$ ,  $R_{yy}$ ,  $R_{xy}$ , and  $R_{yx}$  components of the density matrix will be multiplied by these coefficients. The two files named `table1-1.txt`, `table2-2.txt` have to be present in the directory of the executable main program, exactly as in the case of Tauola++ universal interface [26]. If the tables are absent, or if their name is distinct, the transverse components of  $R_{ij}$  will be equal to zero.
- At execution stage:  
The method `getZgamParametersTR(RXX, RYY, RXY, RYX)`; can be used to port the numerical values of  $R_{xx}$ ,  $R_{yy}$ ,  $R_{xy}$ ,  $R_{yx}$  to the user program to monitor the values or to modify them by repeating the following:  

```
setZgamMultiplierTR(...);
```

`WT1 = calculateWeightFromParticlesH(...)`; for each individual event. Motivated by the results of our tests, we have chosen  $R_{xy}$  and  $R_{yx}$  to be zero in all DY cases.

### A.2 Electroweak corrections

In Tauola++ universal interface transverse spin effects are activated together with electroweak corrections of the SANC library, see Ref. [31]. Now, this is the case in TauSpinner as well. The  $R_{xx}$  and  $R_{yy}$  components of  $\tau^+\tau^-$  pair spin density matrix have been ported to the TauSpinner code. Other, non-diagonal components, have been demonstrated to be suppressed to, or below the few percent level and are not taken into account. See the plots of the file `CPtests/Z-pi/Rijs-INTcosthe.root` discussed in the main body of the paper.

### A.3 Installation

As auxiliary material to this paper, the directory `TAUOLA/TauSpinner/examples/CP-tests` has been prepared. The main program `CP-test.cxx` is based on the default example program `tau-reweight-test.cxx` located in the `TAUOLA/TauSpinner/examples` directory. In order to compile it one has to:

- Configure Tauola++ for compilation with TauSpinner, HepMC [45] and MC-TESTER [44]. See [26] and [12] for instructions on how to define the appropriate paths.
- If using Tauola++ distribution tarball for LCG,<sup>11</sup> available on the project website [47], no additional configuration is required. In case of complete distribution,<sup>12</sup> execute `./configure` with appropriate paths in the `TauSpinner/examples` directory.
- Execute `make` in `CP-tests`.

The example located in this directory is prepared to work without modifications. Please see comments in the code for possible options.

#### A.4 Executing tests

The directory `CP-tests` contains four tests located in sub directories `H-rho`, `H-pi`, `Z-rho` and `Z-pi`. Each test can be executed by the command `../CP-test.exe` in one of those sub directories. Each sub directory contains a small HepMC file `events.dat` with a sample of 100 events to test the installation. See Appendix A.6 for instructions on how to set up generation of larger data samples using Tauola++ and Pythia8. Executing the program with no parameters will process the predefined `events.dat` sample. Any sample can be processed with:

```
../CP-test.exe <data_sample>
[<optional_events_limit>]
```

For each sub directory, an appropriate MC-TESTER user analysis script is provided. Appropriate parameters are set with the help of `setHiggsParametersTR` and `setZgamMultipliersTR` in the main program `CP-test.cxx` file. Note that sub directories `Z-rho` and `Z-pi` contain previously generated tables of electroweak one loop level results for the quark level differential cross section and  $R_{ij}$ ,<sup>13</sup> which are needed for these tests (see Appendix A.2).

For tests (and for our figures), MC-TESTER compares results from processing samples of 1M events for  $pp@8\text{TeV}$  (or  $@14\text{TeV}$ ) collisions generated with Pythia8 [48] hard process option `HiggsSM:ffbar2H` (`WeakSingleBoson:ffbar2gmZ`) turned on. We have

also checked that variation of the Higgs mass in range 120–125 GeV does not affect results beyond the statistical fluctuations. This applies to the case when ISR, FSR is activated in Pythia as well.<sup>14</sup> We have used LHAPDF dataset `cteq6ll.LHpdf` [38]. MC-TESTER user analysis scripts are adapted to the appropriate Higgs ( $Z/\gamma^*$ ) states.

#### A.5 Analyzing results

The result of the test described in previous section is stored in `mc-tester.root` file. It contains all plots defined in user analysis script file.<sup>15</sup> To compare two MC-TESTER root files use `compare.sh` located in the `CP-tests` directory:

```
./compare.sh <file1.root> <file2.root>
```

The benchmark distributions will be stored in the section `USER HISTOGRAMS` of the booklet `tester` produced during comparison. Each directory provides one or more benchmark files that can be used if no changes have been introduced to user analysis script files.

Executing the program in the directory `CP-tests/H-rho` generates Fig. 2 if root files `scalar.root`, `thet-0.2.root` are used as inputs. With `scalar-tauframe.root`, `thet-0.2tauframe.root` used as inputs, the plots for Fig. 3 are generated instead. These plots, to a large degree, coincide with Fig. 2 of Ref. [17]. Note the different choice of quantization frames used in these papers. If the directory `CP-tests/H-pi` is used, Fig. 1 is generated, reproducing Fig. 3 from [16] (files `scalar.root`, `pseudoscalar.root` are used). Not only the acollinearity of  $\pi^\pm$  directions in the rest frame of the Higgs is histogrammed, but also the acoplanarity angle for the  $\pi^-\tau^-$  and  $\pi^+\tau^+$  planes of the same frame (it is not included in our paper).

Numerical results for the DY sample of 1M events are collected in the files: `start60.root` and `transverse60.root` in the `CP-tests/Z-pi` sub directory, and were used for the plot shown in Fig. 4 for the case with the selection  $|\cos\theta_{planes}| > 0.5$ ; files `start60-noc.root` and `transverse60-noc.root` without this selection.

<sup>11</sup> With fixed initialization for  $\tau$  decay matrix elements and prepared for installation in LCG library [46].

<sup>12</sup> Enabling, in particular, the change of  $\tau$  decay matrix elements.

<sup>13</sup> See `Z-pi/table1-1.txt`, `Z-pi/table2-2.txt`. Sub directory `Z-rho` contains symbolic links to these two files. See [26] for instructions on how to generate these tables with modified parametrization.

<sup>14</sup> In this case, a large number of final states can be recognized by MC-TESTER – result of FSR activity in Z or H decays. On some platforms, for bigger samples, this may cause buffer overflow problems. Our examples are not expected to work for all possible options of constructing and storing the event records. They are supposed to work for the properly prepared data files only.

<sup>15</sup> User analysis ROOT scripts are the `.C` files located in the directory where the test is run. The name of those files ends with `*UserTreeAnalysis.C`. Plot definitions located in these files can be modified as needed, however new plot definitions mean that benchmark files provided with the distribution cannot be used for comparison. Keep in mind that in order for MC-TESTER to work correctly `$(MCTESTERLOCATION)` environmental variable must be set.

## A.6 Generating data files

In this section we describe how data files can be generated for the tests. For this purpose, a sub directory CP-tests/generate-datafiles has been provided with a program specifically configured for generating data files for these tests. Note that using this sub directory requires a path to Pythia8 to be provided during the configuration of Tauola++ in addition to other paths.<sup>16</sup> To compile this program, execute “make generate” in the CP-tests directory. To run it, execute:

```
./generate.exe <output_file> <pythia8_config>
<decay_channel> <events_count>
```

Two Pythia8 config files have been prepared: pythia.Z.conf, pythia.H.conf, and they can be used in combination with Tauola++ decay channel 3 or 4 to provide samples for  $\pi$  or  $\rho$  respectively.<sup>17</sup>

The program is set up to strip event of all particles other than  $H$  or  $Z$  boson,  $\tau$  and  $\tau$  decay products. This information is enough for TauSpinner to work and output files are relatively small (around 4 GB per 1M events).

## References

1. ATLAS Collaboration, Phys. Lett. B **716**, 1 (2012). [arXiv:1207.7214](#)
2. CMS Collaboration, Phys. Lett. B **716**, 30 (2012). [arXiv:1207.7235](#)
3. F. Englert, R. Brout, Phys. Rev. Lett. **13**, 321 (1964)
4. P. Higgs, Phys. Rev. Lett. **12**, 132 (1964)
5. ATLAS Collaboration, Phys. Lett. B **726**, 88 (2013). [arXiv:1307.1427](#)
6. CMS Collaboration, JHEP **1306**, 081 (2013). [arXiv:1303.4571](#)
7. ATLAS Collaboration, Phys. Lett. B **726**, 120 (2013). [arXiv:1307.1432](#)
8. CMS Collaboration, Phys. Rev. Lett. **110**, 081803 (2013). [arXiv:1212.6639](#)
9. ATLAS Collaboration, ATLAS-CONF-2014-061 (2014). <http://cds.cern.ch/record/1954724>
10. CMS Collaboration, JHEP **1405**, 104 (2014). [arXiv:1401.5041](#)
11. R. Harnik et al., Phys. Rev. D **88**(7), 076009 (2013). [arXiv:1308.1094](#) [hep-ph]
12. Z. Czyżula, T. Przedzinski, Z. Was, Eur. Phys. J. C **72**, 1988 (2012). [arXiv:1201.0117](#)
13. S. Banerjee et al., Eur. Phys. J. C **73**, 2313 (2013). [arXiv:1212.2873](#)
14. A. Kaczmarek et al., Acta Phys. Polon. **45**, 1921 (2014). [arXiv:1402.2068](#)
15. J.R. Dell’Aquila, C.A. Nelson, Nucl. Phys. B **320**, 86 (1989)
16. M. Kramer et al., Z. Phys. C **64**, 21 (1994). [hep-ph/9404280](#)
17. K. Desch et al., Phys. Lett. B **579**, 157 (2004). [hep-ph/0307331](#)
18. Y.-S. Tsai, Phys. Rev. D **4**, 2821 (1971)
19. G. Bower et al., Phys. Lett. B **543**, 227 (2002). [hep-ph/0204292](#)
20. K. Desch, Z. Was, M. Worek, Eur. Phys. J. C **29**, 491 (2003). [hep-ph/0302046](#)
21. A. Rouge, Phys. Lett. B **619**, 43 (2005). [hep-ex/0505014](#)
22. B. Gripaios et al., JHEP **1303**, 106 (2013). [arXiv:1210.1938](#) [hep-ph]
23. M. Davier et al., Phys. Lett. B **306**, 411 (1993)
24. S. Berge, W. Bernreuther, J. Ziethe, Phys. Rev. Lett. **100**, 171605 (2008). [arXiv:0801.2297](#) [hep-ph]
25. P. Golonka et al., Comput. Phys. Commun. **174**, 818 (2006). [hep-ph/0312240](#)
26. N. Davidson et al., Comput. Phys. Commun. **183**, 821 (2012). [arXiv:1002.0543](#)
27. S. Jadach et al., Acta Phys. Polon. B **43**, 2067 (2012). [arXiv:1209.4291](#)
28. A. van Hameren, Z. Was, Eur. Phys. J. C **61**, 33 (2009). [arXiv:0802.2182](#)
29. S. Alioli, P. Nason, C. Oleari, E. Re, JHEP **0904**, 002 (2009). [arXiv:0812.0578](#)
30. P. Nason, C. Oleari, JHEP **1002**, 037 (2010). [arXiv:0911.5299](#)
31. A. Andonov et al., Comput. Phys. Commun. **181**, 305 (2010). [arXiv:0812.4207](#)
32. S. Jadach, Z. Was, Acta Phys. Polon. B **15**, 1151 (1984) [Erratum: B **16**, 483 (1985)]
33. S. Jadach, J.H. Kühn, Z. Was, Comput. Phys. Commun. **64**, 275 (1990)
34. S. Jadach, B. Ward, Z. Was, Comput. Phys. Commun. **130**, 260 (2000). [hep-ph/9912214](#)
35. S. Jadach, B. Ward, Z. Was, Comput. Phys. Commun. **79**, 503 (1994)
36. S. Jadach, B. Ward, Z. Was, Eur. Phys. J. C **22**, 423 (2001). [hep-ph/9905452](#)
37. M.R. Whalley, D. Bourilkov, R.C. Group, The Les Houches accord PDFs (LHAPDF) and LHAGLUE. Contributed to HERA and the LHC: a workshop on the implication conference. [arXiv:hep-ph/0508110](#)
38. LHAPDF website. <http://projects.hepforge.org/lhapdf/>. Accessed 21 Nov 2014
39. Z. Was, S. Jadach, Phys. Rev. D **41**, 1425 (1990)
40. N. Davidson, T. Przedzinski, Z. Was, PHOTOS interface in C++: technical and physics documentation. [arXiv:1011.0937](#)
41. S. Berge, W. Bernreuther, Phys. Lett. B **671**, 470 (2009). [arXiv:0812.1910](#)
42. S. Berge, W. Bernreuther, S. Kirchner, [arXiv:1408.0798](#) [hep-ph]
43. J. Kalinowski, Z. Was, in preparation
44. N. Davidson et al., Comput. Phys. Commun. **182**, 779 (2011). [arXiv:0812.3215](#)
45. M. Dobbs, J.B. Hansen, Comput. Phys. Commun. **134**, 41 (2001). <https://savannah.cern.ch/projects/hepmc/>
46. LCG project. <http://service-spi.web.cern.ch/service-spi/external/MCGenerators/>. Accessed 21 Nov 2014
47. Tauola++ website. <http://web.cern.ch/taulapp/>. Accessed 21 Nov 2014
48. T. Sjöstrand, S. Mrenna, P. Skands, Comput. Phys. Commun. **178**, 852 (2008). [arXiv:0710.3820](#)

<sup>16</sup> Contrary to TAUOLA/examples sub directory, this program is set up only for pythia version 8.180 or later. When using older versions, changes to the use of pythia8 HepMC interface may have to be introduced.

<sup>17</sup> Tests described in this paper have been configured for proton-proton collisions at  $\sqrt{s} = 14$  TeV, therefore Pythia8 configuration files use the same setup.